

Organotin(IV) derivatives of *o*-isobutyl carbonodithioate: Synthesis, spectroscopic characterization, X-ray structure, HOMO/LUMO and *in vitro* biological activities



Fatima Javed^a, Muhammad Sirajuddin^{b,*}, Saqib Ali^{a,*}, Nasir Khalid^c, Muhammad Nawaz Tahir^d, Naseer Ali Shah^e, Zahid Rasheed^a, Muhammad Rashid Khan^f

^a Department of Chemistry, Quaid-i-Azam University, Islamabad 45320, Pakistan

^b Department of Chemistry, University of Science & Technology, Bannu, Pakistan

^c Chemistry Division, Pakistan Institute of Nuclear Science and Technology, P.O. Nilore, Islamabad, Pakistan

^d Department of Physics, University of Sargodha, Pakistan

^e Department of Biosciences, COMSATS Institute of Information Technology, Islamabad, Pakistan

^f Department of Biochemistry, Quaid-i-Azam University, Islamabad 45320, Pakistan

ARTICLE INFO

Article history:

Received 17 September 2015

Accepted 15 November 2015

Available online 2 December 2015

Keywords:

Organotin(IV) complex

HOMO–LUMO calculation

DNA interaction

In vitro biological application

Protein kinase inhibition

ABSTRACT

A series of organotin(IV) complexes have been synthesized by reacting potassium *o*-isobutyl carbonodithioate with di- and triorganotin halides in methanol under stirring conditions. The newly synthesized complexes have been characterized by elemental analysis, FT-IR, NMR (¹H and ¹³C) and X-ray crystallography. The FT-IR results show that the ligand acts as bidentate in complexes **1–3** and monodentate in complexes **4** and **5**, which were also confirmed by theoretical calculations. The NMR data reveal four and six coordinated geometries in solution. A HOMO–LUMO study shows that all the complexes are stable. Biological screenings demonstrate that, with a few exceptions, all the complexes show significant activity against various bacterial and fungal strains. The synthesized complexes were also found to be effective antioxidants of the 2,2-diphenyl-1-picrylhydrazyl radical (DPPH). All the complexes have been assayed for antileishmanial activity *in vitro* and found some promising results. The UV–Vis studies confirmed that the ligand and its complexes bind to DNA *via* intercalative interactions, resulting in hypochromism and minor red shifts.

© 2015 Published by Elsevier Ltd.

1. Introduction

The multifunctional approaches of dithiocarbonates make its chemistry more impressive due to its chemical interaction with a variety of biomolecules, such as proteins, DNA and drugs etc. One of the important structural consequences of dithio ligands lead to the preferential stabilization of specific stereochemistries in their metal complexes. Dithio ligands are considered as soft donors, showing excellent coordination ability. They form stable complexes with transition as well as non-transition metal ions [1,2] and exhibit a variety of coordination modes in homo and heteronuclear complexes, depending on the binding modes of the ligands toward the metal center [3–7]. Subsequently, extensive structural analyses were performed by Tiekink and Haiduc [8]

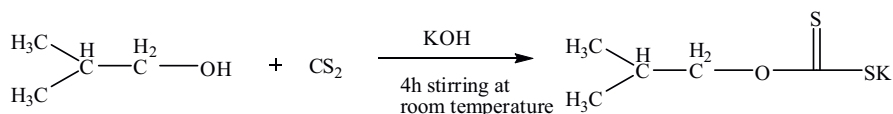
which showed that these ligands can coordinate to metal atoms in monodentate, isobidentate or anisobidentate fashions. More recent applications of xanthates and other thio-compounds are in the production of nanoparticles of metal sulfides [9,10] and for the use of their non-linear optical properties [11,12]. Metal xanthates are extensively used as pesticides [13], corrosion inhibitors [14], agricultural reagents [15] and quite recently in therapy for HIV infections [16]. Moreover, xanthates are also known to show antitumor properties [17,18] and their antioxidant properties could be of importance for treating Alzheimer's disease [19].

The chemistry of organotin compounds is gaining attention on account of their interesting structural features, schizonticidal, anti-malarial, fungicidal activities and their potential as agricultural biocides [20]. Recent studies have shown very promising *in vitro* antitumor properties of organotin compounds against a wide panel of tumor cell lines of human origin. In some cases, organotin(IV) derivatives have also shown acceptable antiproliferative *in vivo* activity as new chemotherapy agents. The biological activity of

* Corresponding authors. Tel.: +92 5190642130; fax: +92 5190642241.

E-mail addresses: m.siraj09@yahoo.com (M. Sirajuddin), drsa54@hotmail.com (S. Ali).

organotin compounds is basically determined by the number and nature of the organic groups bound to the central tin atom. $[R_3Sn(IV)]^+$ and $[Ar_3Sn(IV)]^+$ derivatives exert powerful toxic action on the central nervous system. Within the series of $[R_3Sn(IV)]^+$ compounds, the lower homologs (Me, Et) are the most toxic when administered orally, and the toxicity reduces progressively on going from propyl to octyl, the latter not being toxic at all. The presence of easily hydrolysable groups (easily dissociable chelating ligands), producing intermediates such as $R_nSn^{(4-n)+}$ ($n = 2$ or 3) moieties which may bind with DNA or the high affinity site of ATPase (histidine only), the low-affinity site of ATPase and hemoglobins (histidine and cystine), play an important role in the determination of the biological activity of the organotin compounds. Therefore, substantial attempts have been made to characterize model organotin compounds of ligands having hetero donor atoms



(O, N and S), and simultaneously several studies have been focused on structure–activity correlations during the last two decades [21].

In the present study we have synthesized some novel organotin complexes by the reaction of di- and triorganotin(IV) halides with a sulfur donor ligand. The complexes have been characterized by FT-IR, NMR (^1H and ^{13}C), X-ray crystallography and a computational study. A HOMO/LUMO study was performed to establish the stability of the complexes. Biological screening, *i.e.* antibacterial, antifungal, antileishmanial, antioxidant, toxicity, protein kinase inhibition and DNA binding studies, have been performed to establish the significance of the synthesized complexes.

2. Experimental

2.1. Materials and methods

All the organotin(IV) halides, Ph_3SnCl , isobutanol, potassium hydroxide and carbon disulfide were obtained from Aldrich (USA) and were used without further purification. All the solvents purchased from E. Merck (Germany) were dried before use according to literature procedures [22]. Melting points were recorded with a Bio-Cote Model SMP10 melting point apparatus and are uncorrected. FT-IR spectra were recorded in the range $4000\text{--}250\text{ cm}^{-1}$ with a Thermo Scientific Nicolet-6700 FTIR spectrometer and NMR spectra were obtained with a Bruker Avance 300 MHz NMR spectrometer. Absorption spectra were measured on a double beam UV-Vis spectrometer, Shimadzu 1800, at $25 \pm 1^\circ\text{C}$. The sodium salt of DNA (Acros) was used as received. The quantitative determination of C, H and S was carried out using a LECO CHNS-932 analyzer. The X-ray diffraction data were collected on a Bruker SMART APEX CCD diffractometer, equipped with a 4 K CCD detector set 60.0 mm from the crystal. The crystals were cooled to $100 \pm 1\text{ K}$ using a Bruker KRYOFLEX low temperature device and intensity measurements were performed using graphite monochromated Mo K α radiation from a sealed ceramic diffraction tube (SIEMENS). The structure was solved by the Patterson method and extension of the model was accomplished by the direct method using the program DIRDIF or SIR2004. Final refinement on F2 was carried out by full matrix least squares techniques using SHELXL-97, a modified version of the program PLUTO (to prepare illustrations) and the PLATON package.

2.2. Synthesis

2.2.1. Synthesis of the ligand (KL)

Potassium *o*-isobutyl carbonodithioate was prepared by stirring equimolar amounts (1 mmol) of isobutanol, potassium hydroxide and carbon disulfide (1 mmol) with continuous stirring at ambient temperature ($23 \pm 1^\circ\text{C}$) for 4 h. The precipitates obtained were filtered off and dried in air.

Yield: 92%. M.p.: $205\text{--}206^\circ\text{C}$. Mol. Wt.: 187.97. Anal. Calc. for $\text{C}_5\text{H}_9\text{KOS}_2$: C, 31.88 (31.84); H, 4.82 (4.85); S, 34.05 (34.02). IR (cm^{-1}): 997 $\nu(\text{C}=\text{O})$; 1396 $\nu(\text{CSSasym})$; 1124 $\nu(\text{CSSsym})$; 272 ($\Delta\nu$); ^1H NMR (DMSO- d_6 , 300 MHz) δ (ppm): 0.87 (d, 6H, H1, $^3J[^1\text{H}, ^1\text{H}] = 6.6\text{ Hz}$); 1.90 (m, ^1H , H2); 3.96 (d, 2H, H3, $^3J[^1\text{H}, ^1\text{H}] = 6.6\text{ Hz}$). ^{13}C NMR (DMSO- d_6 , 75 MHz) δ (ppm): 19.9 (C1); 27.9 (C2); 77.6 (C3); 230.5 (C4).

2.2.2. Synthesis of the organotin(IV) complexes

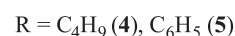
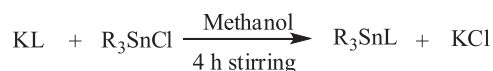
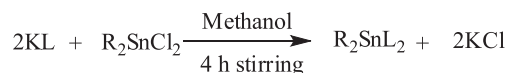
Potassium *o*-isobutyl carbonodithioate (2 mmol) was dissolved in methanol (20 mL) in a round bottom two-necked flask (100 mL) with continuous stirring at ambient temperature. Then to this solution, $\text{R}_2\text{SnCl}_2/\text{R}_3\text{SnCl}$ (1 mmol/2 mmol) was added. The reaction mixture was continuously stirred for 4 h at room temperature. The solvent was evaporated slowly at room temperature. The solid product obtained was dried in air and recrystallized from an acetone:ether mixture (1:1). The synthesis of the organotin(IV) complexes have been shown as a generalized chemical equation in Scheme 1, whereas the numbering patterns of KL and the alkyl groups attached to the Sn atom for NMR interpretation are depicted in Scheme 2.

2.2.3. Dimethylstannanediyl bis (*o*-isobutyl dicarbonodithioate) (1)

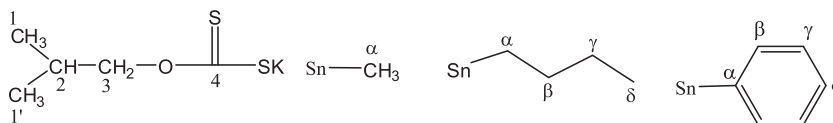
Yield: 86%. M.p. $105\text{--}106^\circ\text{C}$. Mol. Wt.: 447.97. Anal. Calc. for $\text{C}_{12}\text{H}_{24}\text{O}_2\text{S}_4\text{Sn}$: C, 32.22 (32.19); H, 5.41 (5.38); S, 25.68 (25.65). IR (cm^{-1}): 961 $\nu(\text{C}=\text{O})$; 1259 $\nu(\text{CSSasym})$; 1078 $\nu(\text{CSSsym})$; 181 ($\Delta\nu$); 377 $\nu(\text{Sn}=\text{S})$; 557 $\nu(\text{Sn}=\text{C})$. ^1H NMR (DMSO- d_6 , 300 MHz) δ (ppm): 1.01 (d, 12H, H1, $^3J[^1\text{H}, ^1\text{H}] = 6.6\text{ Hz}$); 2.15 (m, 2H, H2); 4.23 (d, 4H, H3, $^3J[^1\text{H}, ^1\text{H}] = 6.6\text{ Hz}$), 1.51 (s, 6H, H α) [$^{119/117}\text{Sn} - ^1\text{H}$] = 79, 76 Hz). ^{13}C NMR (DMSO- d_6 , 75 MHz) δ (ppm): 19.0 (C1); 27.7 (C2); 82.3 (C3); 222.2 (C4); 10.5 (C α , [$^{119/117}\text{Sn} - ^{13}\text{C}\alpha$] = 599, 573 Hz).

2.2.4. Dibutylstannanediyl bis (*o*-isobutyl dicarbonodithioate) (2)

Yield: 85%. M.p. oily. Mol. Wt.: 532.06. Anal. Calc. for $\text{C}_{18}\text{H}_{36}\text{O}_2\text{S}_4\text{Sn}$: C, 40.68 (40.65); H, 6.83 (6.80); S, 24.13 (24.10).



Scheme 1. Generalized chemical equations for the synthesis of the organotin(IV) derivatives.



Scheme 2. Numbering patterns of KL and the organic moieties attached to the Sn atom for NMR interpretation.

IR (cm^{-1}): 967 $\nu(\text{C}-\text{O})$; 1267 $\nu(\text{CSSasym})$; 1067 $\nu(\text{CSSsym})$; 200 ($\Delta\nu$); 369 $\nu(\text{Sn}-\text{S})$; 558 $\nu(\text{Sn}-\text{C})$; ^1H NMR (DMSO- d_6 , 300 MHz) δ (ppm): 0.99 (d, 12H, H1); 2.14 (m, 2H, H2); 4.24 (d, 4H, H3, $^3J[^1\text{H}, ^1\text{H}] = 6.6$ Hz), 2.03 (m, 4H, H α), 1.88 (m, 4H, H β); 1.43 (m, 4H, H γ); 0.93 (m, 6H, H δ , $^3J[^1\text{H}, ^1\text{H}] = 7.2$ Hz). ^{13}C NMR (DMSO- d_6 , 75 MHz) δ (ppm): 19.2 (C1); 26.4 (C2); 82.1 (C3); 223.2 (C4); 30.5 (C α , $^1J[^{119/117}\text{Sn}-^{13}\text{C}\alpha] = 542$, 518 Hz); 29.0 (C β , $^2J[^{119/117}\text{Sn}-^{13}\text{C}\beta] = 39$ Hz); 27.7 (C γ , $^3J[^{119/117}\text{Sn}-^{13}\text{C}\gamma] = 39$, 35 Hz); 13.7 (C δ).

2.2.5. Diphenylstannediyl bis (o-isobutyl dicarbonodithioate) (3)

Yield: 76%. M.p. 90–91 °C. Mol. Wt.: 572.0. Anal. Calc. for $\text{C}_{22}\text{H}_{28}\text{O}_2\text{S}_4\text{Sn}$: C, 46.24 (46.21); H, 4.94 (4.90); S, 22.45 (22.42). IR (cm^{-1}): 944 $\nu(\text{C}-\text{O})$; 1251 $\nu(\text{CSSasym})$; 1045 $\nu(\text{CSSsym})$; 206 ($\Delta\nu$); 370 $\nu(\text{Sn}-\text{S})$; 283 $\nu(\text{Sn}-\text{C})$. ^1H NMR (DMSO- d_6 , 300 MHz) δ (ppm): 0.89 (d, 12H, H1, $^3J[^1\text{H}, ^1\text{H}] = 6.6$ Hz); 1.90 (m, 2H, H2); 4.15 (m, 4H, H3); 7.74 (m, 4H, H β); 7.49 (m, 4H, H γ); 7.47 (m, 2H, H δ). ^{13}C NMR (DMSO- d_6 , 75 MHz) δ (ppm): 19.0 (C1); 27.5 (C2); 82.7 (C3); 215.7 (C4); 130.0 (C α , $^1J[^{119/117}\text{Sn}-^{13}\text{C}\alpha] = 828$, 793 Hz), 128.7 (C β , $^2J[^{119/117}\text{Sn}-^{13}\text{C}\beta] = 71$, 68 Hz); 135.5 (C γ , $^3J[^{119/117}\text{Sn}-^{13}\text{C}\gamma] = 55$, 52 Hz); 131.0 (C δ , $^4J[^{119/117}\text{Sn}-^{13}\text{C}\delta] = 15$ Hz).

2.2.6. Tributylstannyl o-isobutylcarbonodithioate (4)

Yield: 80%. M.p. oily. Mol. Wt.: 440.12. Anal. Calc. for $\text{C}_{17}\text{H}_{36}\text{OS}_2\text{Sn}$: C, 46.48 (46.45); H, 8.26 (8.24); S, 14.60 (14.56). IR (cm^{-1}): 960 $\nu(\text{C}-\text{O})$; 1288 $\nu(\text{CSSasym})$; 1021 $\nu(\text{CSSsym})$; 267 ($\Delta\nu$); 366 $\nu(\text{Sn}-\text{S})$; 592 $\nu(\text{Sn}-\text{C})$; ^1H NMR (DMSO- d_6 , 300 MHz) δ (ppm): 0.98 (d, 6H, H1, $^3J[^1\text{H}, ^1\text{H}] = 6.6$ Hz); 2.12 (m, 2H, H2); 4.23 (m, 4H, H3, $^3J[^1\text{H}, ^1\text{H}] = 6.6$ Hz); 1.61 (m, 6H, H α), 1.38 (m, 6H, H β); 1.33 (m, 6H, H γ); 0.91 (m, 9H, H δ , $^3J[^1\text{H}, ^1\text{H}] = 7.2$ Hz). ^{13}C NMR (DMSO- d_6 , 75 MHz) δ (ppm): 19.2 (C1); 27.6 (C2); 81.3 (C3); 218.3 (C4); 15.8 (C α , $^1J[^{119/117}\text{Sn}-^{13}\text{C}\alpha] = 337$, 322 Hz), 29.0 (C β , $^2J[^{119/117}\text{Sn}-^{13}\text{C}\beta] = 22$ Hz); 27.0 (C γ , $^3J[^{119/117}\text{Sn}-^{13}\text{C}\gamma] = 66$, 63 Hz); 13.6 (C δ).

2.2.7. Triphenylstannyl o-isobutylcarbonodithioate (5)

Yield: 91%. M.p. 111–112 °C. Mol. Wt.: 500.03. Anal. Calc. for $\text{C}_{23}\text{H}_{24}\text{OS}_2\text{Sn}$: C, 55.33 (55.31); H, 4.85 (4.80); S, 12.84 (12.81). IR (cm^{-1}): 996 $\nu(\text{C}-\text{O})$; 1297 $\nu(\text{CSSasym})$; 1044 $\nu(\text{CSSsym})$; 253 ($\Delta\nu$); 375 $\nu(\text{Sn}-\text{S})$; 279 $\nu(\text{Sn}-\text{C})$. ^1H NMR (DMSO- d_6 , 300 MHz) δ (ppm): 0.90 (d, 6H, H1, $^3J[^1\text{H}, ^1\text{H}] = 6.6$ Hz); 1.90 (m, 2H, H2); 4.09 (m, 4H, H3, $^3J[^1\text{H}, ^1\text{H}] = 6.6$ Hz); 8.02 (m, 6H, H β); 7.51 (m, 6H, H γ); 7.49 (m, 3H, H δ). ^{13}C NMR (DMSO- d_6 , 75 MHz) δ (ppm): 19.3 (C1); 29.7 (C2); 83.0 (C3); 218.7 (C4); 139.0 (C α , $^1J[^{119/117}\text{Sn}-^{13}\text{C}\alpha] = 566$, 543 Hz), 128.6 (C β , $^2J[^{119/117}\text{Sn}-^{13}\text{C}\beta] = 59$, 57 Hz); 136.6 (C γ , $^3J[^{119/117}\text{Sn}-^{13}\text{C}\gamma] = 44$ Hz); 129.4 (C δ , $^4J[^{119/117}\text{Sn}-^{13}\text{C}\delta] = 13$ Hz).

2.3. Theoretical study

All the calculations were performed using the 6-31G* basis set for H, C, O and S. This is a split valence double-zeta basis set which adds d-type polarization functions on the first and second row elements. For the Sn atom, the LANL2DZ basis set was used, which uses the Los Alamos effective core potential on the metal atom. The geometries of complexes **1–5** were optimized with the DFT/B3LYP method as implemented in the Gaussian-09 quantum chemistry package [23]. In the geometry optimization procedure, no

symmetry restrictions were imposed on any complex. The Hessian calculations confirmed that the optimized structures are local minima on the potential energy surface as no imaginary frequencies were found in any case. The plots of the optimized structures and the HOMO–LUMO were realized, respectively, with Molden [24] and CCP1-GUI [25] programs.

2.4. Biological screenings

DNA interaction assay by UV–Vis spectroscopy, antibacterial, antifungal, antileishmanial, antioxidant, cytotoxicity and protein kinase inhibition studies were performed using the same procedures as reported earlier [26,27].

3. Results and discussion

The proposed chemical structures of the synthesized complexes are given in Supplementary data Table S1.

3.1. FT-IR spectra

The characteristic IR frequencies (cm^{-1}) of the ligand (KL) and its organotin(IV) complexes (**1–5**) are listed in the experimental part. Several significant changes on complexation with respect to the bands of the free ligand suggest coordination through the thio-carboxylate group of the ligand. In the spectra of the investigated complexes, the vibrational modes of CS_2 are of particular interest to differentiate between monodentate and bidentate coordination of the dithiolate moiety. The FT-IR spectra of complexes **1–5** gave strong peaks at 1251–1297 cm^{-1} , attributed to the asymmetric $\nu(\text{CS}_2)_{\text{as}}$ absorption, and 1021–1078 cm^{-1} , assigned to symmetric $\nu(\text{CS}_2)_{\text{s}}$ absorption frequencies. The differences between $\nu(\text{CS}_2)_{\text{as}}$ and $\nu(\text{CS}_2)_{\text{s}}$ are 181, 200 and 206 cm^{-1} for complexes **1–3**, respectively, which indicate a bidentate binding mode of the ligand to the central tin atom. For complexes **4** and **5**, the differences are 267 and 253 cm^{-1} , which indicate a monodentate mode, probably due to steric effects [28]. The binding modes of the complexes were also confirmed by a theoretical study. The FT-IR results of complex **1** are consistent with the X-ray crystallographic data. The IR bands observed in the range 366–377 cm^{-1} in the spectra of the complexes are assigned to Sn–S bonding [29]. The absorptions at 557, 558 and 592 cm^{-1} are assigned to $\nu(\text{Sn}-\text{C})$ bands for complexes **1**, **2** and **4**, respectively whereas for the di- and triphenyltin(IV) derivatives (**3** and **5**), the $\nu(\text{Sn}-\text{C})$ bands are observed at 283 and 279 cm^{-1} , respectively. These values are in close agreement with those observed for a number of organotin(IV) derivatives of sulfur donor ligands [28]. Based on the infrared analyses, it is suggested that the ligand is coordinated to the tin(IV) moiety through the thiolato sulfur atoms.

3.2. ^1H and ^{13}C NMR spectra

In the ^1H NMR spectra, the chemical shifts were identified from their relative intensities and multiplicity patterns. The total numbers of protons, calculated from the integration curves, are compatible with the proposed structures. The protons H1, H2 and H3 of the ligand appeared at 0.87, 1.90 and 3.96 ppm and these peaks exhibited a downfield shift in the complexes (**1–5**) in the range

Table 1
(C–Sn–C) angles (°) based on NMR parameters of complexes **1–5**.

Compd. no.	1J [^{119}Sn , ^{13}C] (Hz)	2J [^{119}Sn , ^1H] (Hz)	Angles (°)	
			1J	2J
1	599	80	129	126
2	542	–	128	–
3	828	–	128	–
4	337	–	108	–
5	566	–	111	–

0.89–1.01 for H1, 2.12–2.15 for H2 and 4.09–4.24 ppm for H3. This downfield shift is due to the deshielding of these protons due to deprotonation of the ligand and coordination of the CS_2 group to the tin moiety. These observations are in agreement with the reported triphenyltin(IV) dithiocarboxylates [30]. The coupling constant [2J (^{119}Sn , ^1H)] for **1** was 79 Hz, which is in the expected range for a six-coordinated Sn center and is consistent with a C–Sn–C angle of 126° . The coupling constants, [2J (^{119}Sn , ^1H)], for the *n*-butyl-, di-, and triphenyltin(IV) complexes could not be determined owing to their complex patterns. The geometry of the triphenyltin(IV) complex was calculated from the difference in the chemical shift resonances of the ortho to meta and para protons (0.5 ppm), which matched well with the bidentate bonding of the 1,1-dithiolate moiety in solution [31].

The ^{13}C NMR spectral data, along with the assignment of characteristic peaks of the ligand and the organotin(IV) complexes, are described in the experimental section. An important chemical shift of a carbon atom in the dithiocarbonate complex is that of the thione carbon (CS_2). The signal due to the CS_2 carbon atom in the free ligand appears at 230.5 ppm. However, in the spectra of the corresponding tin complexes, this appears at 222.2 in complex **1**, 223.2 in **2**, 215.7 in **3**, 218.3 in **4** and 218.7 ppm in **5**, indicating

the coordination of the ligand to the metal center *via* the $-\text{CSS}$ moiety [30]. Coordination of the Sn atom in the di- and triorganotin complexes has been further supported by the 1J (^{119}Sn – ^{13}C) coupling constants and the C–Sn–C angles (108 – 129°), calculated by Lockhart's equation (Table 1) [32]. In complexes **1–3**, the 1J (^{119}Sn – ^{13}C) coupling constants observed and C–Sn–C angles calculated were 599 Hz (129°), 542 Hz (128°) and 828 Hz (128°), which are attributed to a six coordinated geometry, while a four coordinated geometry is inferred for complexes **4** and **5**, having coupling constants and angles of 337 Hz (108°) and 566 Hz (111°) [33]. This was further confirmed by theoretical calculations. The results are also consistent with the X-ray crystallographic structure for complex **1**.

3.3. Crystal structure of complex **1**

The structure of complex **1** and its packing diagrams are shown in Figs. 1–3. The crystal and structural refinement data and selected interatomic parameters are summarized in Tables 2 and 3, respectively. The Sn atom is coordinated by two methyl groups and two dithiocarboxylate ligands, with the latter adopting similar behavior with regard to their coordination modes. The two ligands are anisobidentically chelated to Sn, with one longer Sn–S2 and one shorter Sn–S1 bond (3.125(15) and 2.481(14) Å). The longer Sn–S distances are significantly less than the sum of the van der Waal's radii (4.0 Å), and the coordination number of Sn is unambiguously assigned as six. The overall geometry at Sn is, however, highly distorted from *trans* octahedral: the C6–Sn–C7 angle is only $134.5(5)^\circ$, the Sn and four sulfur atoms of the dithiocarboxylate ligands are nearly coplanar, but are badly distorted from a square-planar geometry (the *cis* (S–Sn–S) angles range from $85.7(6)$ [S1–Sn–S1A] to $146.9(1)^\circ$ [(S2–Sn–S2A)]. In both anisobidentate ligands, each shorter Sn–S bond is associated with a longer

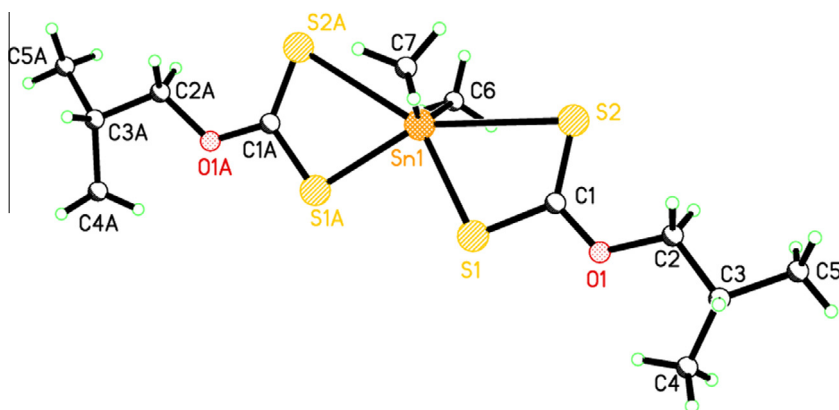


Fig. 1. Crystal structure of complex **1**.

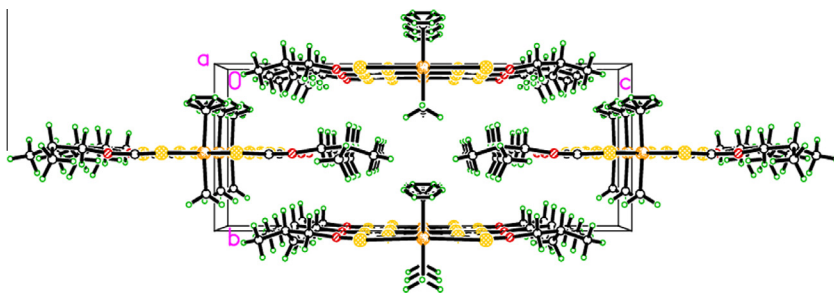


Fig. 2. Packing diagram of complex **1** viewed along the *a*-axis.

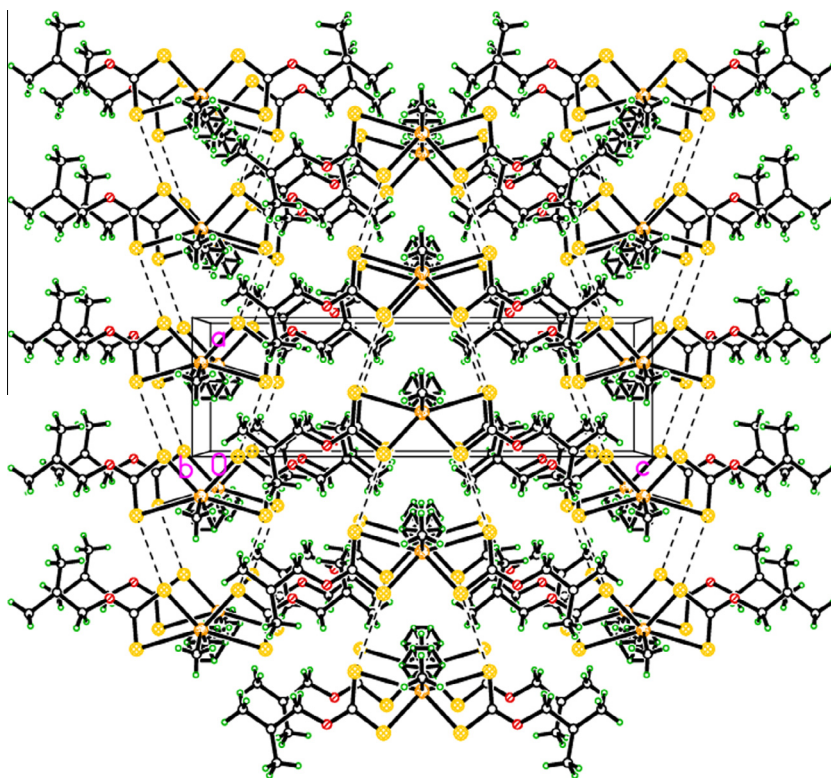


Fig. 3. Packing diagram of complex **1** viewed along the *b*-axis. Dotted lines show the intramolecular interactions.

C–S bond and *vice versa*, which is in consonance with the bonding asymmetry of the ligands. The bond angles subtended at the Sn atom by the methyl carbons (C6 and C7) and S1 and S1A atoms range from 107.5(6) to 105.4(7)°, demonstrating that the Sn–C bonds are bent toward the longer Sn–S bonds. This may be due to repulsion between the bonding electron pairs around the central Sn atom. The geometry and bond lengths of the SnC₂S₄ core are comparable with those observed for analogous complexes [34,35].

3.4. Theoretical calculations

Molecular modelling was used to study the theoretical significant features of the organometallic frameworks, i.e. molecular geometries, bond energies and torsion angles, since it provides a blueprint of the three-dimensional arrangements of atoms [36]. Bond lengths, bond angles and atomic coordinates depend on the hybridization of an atom and the mode of bonding. The molecular structures of complexes **1–5** were optimized by Gaussian 03 using the DFT/B3LYP method to support the spectroscopic data. The selected geometric parameters, viz. bond lengths, bond angles and torsion angles of the optimized structures are summarized in Table 4. The optimized molecular structure, HOMO and LUMO of complexes **1–5** are shown in Figs. 4 and 5. The ligand is coordinated through the thiolic sulfur atoms and act as bidentate in the case of complexes **1, 2** and **3**, showing a distorted octahedral geometry, and monodentate in complexes **4** and **5**, having a tetrahedral geometry instead of a trigonal pyramidal geometry. The bond angles and bond lengths also show distorted octahedral and tetrahedral geometries. The Sn–S bond distance is nearly identical to the values of reported tin complexes. The calculated Sn–S bond distances of complexes **1, 4** and **5** are 2.846, 2.50 and 2.489 Å, which are close to the already reported thiocarboxylates [37]. The bond angles in complex **1** are C(2)–Sn(1)–C(4) = 109.15°, C

(4)–Sn(1)–S(5) = 101.89° and S(3)–Sn(1)–S(5) = 148.21°; in complex **2** C(2)–Sn(1)–C(4) = 111.55°, C(4)–Sn(1)–S(5) = 98.94° and S(3)–Sn(1)–S(5) = 148.08°; in complex **3** C(2)–Sn(1)–C(4) = 105.59°, C(4)–Sn(1)–S(5) = 101.67° and S(3)–Sn(1)–S(5) = 149.08°; in complex **4** C(2)–Sn(1)–C(5) = 116.39°, S(3)–Sn(1)–C(5) = 110.45° and S(3)–Sn(1)–C(4) = 97.37°; in complex **5** C(2)–Sn(1)–C(5) = 114.67°, S(3)–Sn(1)–C(5) = 115.36° and S(3)–Sn(1)–C(4) = 95.95°, which are all in good agreement with the values reported for tin complexes of thiohydrazones [38]. In the investigated complexes **1–5**, the HOMO orbital is primarily located on a sulfur moiety, whereas the LUMO orbital is concentrated on the tin atom, which indicates that it is susceptible to nucleophilic attack. The calculated HOMO and LUMO energies are summarized in Table 5. An electronic system with larger HOMO–LUMO gap should be less reactive than one having a smaller gap. The lower value of the HOMO–LUMO energy gap would explain the eventual charge-transfer interaction taking place within the molecules. In the present study, the HOMO–LUMO gap values of complexes **1–5** are 4.60, 4.483, 4.644, 4.888 and 4.887 eV (Table 5), which show that the complexes are stable [60].

3.5. DNA binding studies

The absorption spectra of the ligand KL and the organotin(IV) thiocarboxylates **1** and **3** in the absence and presence of salmon sperm DNA (SS-DNA) have been recorded at different concentrations of DNA by keeping the concentration of the ligand and organotin(IV) complexes constant. There exists a single absorption band at 308.2, 309.3 and 309.50 nm for KL, **1** and **3** respectively. The ligand KL and complexes **1** and **3** showed a minor bathochromic shift of the spectral band with significant hypochromicity (Figs. 6–8), suggesting groove binding as well as intercalation of the complexes with the DNA helix [39,40]. An isosbestic point near 277 nm was

Table 2
Crystal and structure refinement data for complex 1.

Empirical formula	C ₁₂ H ₂₄ O ₂ S ₄ Sn
Formula weight	447.97
T (K)	296(2)
Crystal system	orthorhombic
Space group	Pn2 ₁ m
a (Å)	6.104(4)
b (Å)	8.058(5)
c (Å)	20.186(5)
α, β, γ (°)	90, 90, 90
V (Å ³)	992.9(9)
Z	2
ρ _{calc} (g cm ⁻³)	1.496
m (mm ⁻¹)	1.703
F(000)	452.0
Crystal size (mm ³)	0.28 × 0.22 × 0.18
Radiation	Mo Kα (λ = 0.71073)
2θ range for data collection	4.036–55.692°
Index ranges	–7 ≤ h ≤ 4, –10 ≤ k ≤ 10, –26 ≤ l ≤ 26
Reflections collected	4871
Independent reflections	2208 [R _{int} = 0.0249, R _{sigma} = 0.0354]
Data/restraints/parameters	2208/7/125
Goodness-of-fit (GOF) on F ²	0.983
Final R indexes [I ≥ 2σ (I)]	R ₁ = 0.0321, wR ₂ = 0.0632
Final R indexes [all data]	R ₁ = 0.0516, wR ₂ = 0.0708
Largest difference in peak and hole (e Å ⁻³)	0.38 and –0.47
Flack parameter	0.41(7)

Table 3
Selected bond lengths (Å) and angles (°) of complex 1.

Selected bond lengths (Å)			
C1–O1	1.304(6)	C6–Sn1	2.08(2)
C1–S1	1.728(5)	C7–Sn1	2.12(2)
C1–S2	1.644(5)	S1–Sn1	2.481(14)
C2–O1	1.461(9)	S2–Sn1	3.125(15)
Selected bond angles (°)			
O1–C1–S1	110.9(3)	C6–Sn1–S1	107.5(6)
O1–C1–S2	125.5(4)	C7–Sn1–S1	105.4(7)
S2–C1–S1	123.4(3)	S1–Sn1–S1	85.68(6)
C1–O1–C2	120.9(5)	O1–C2–C3A	115.1(12)
Sn1–S1–C1	95.19(15)	C2–C3A–C4A	112.6(19)
C6–Sn1–C7	134.5(5)	S2–Sn1–S2A	46.9(1)

observed in the spectrum of complex 3. Spectral changes of this type describe covalent binding of the complex with DNA [41,42]. In order to compare the binding strengths of the ligand–DNA and complex–DNA adducts, the intrinsic binding constant K of the ligand and the organotin(IV) thiocarboxylates **1** and **3** were calculated using the Benesi Hildebrand equation [43].

$$\frac{A_0}{A - A_0} = \frac{\epsilon_G}{\epsilon_{H-G} - \epsilon_G} + \frac{\epsilon_G}{\epsilon_{H-G} - \epsilon_G} \frac{1}{K[\text{DNA}]}$$

where K is the binding constant, A_0 and A are the absorbances of the drug and its complex with DNA, and ϵ_G and ϵ_{H-G} are the Absorption coefficients of the drug and drug–DNA complex, respectively. The binding constants were obtained from the intercept to slope ratios of $A_0/(A - A_0)$ vs. $1/[\text{DNA}]$ plots. The binding constants were determined to be 9.9×10^5 , 2.5×10^5 and $1.1 \times 10^6 \text{ M}^{-1}$ for KL, **1** and **3** respectively, indicating that among the tested complexes, the binding strength of complex 3 with DNA is maximum and that of complex 1 is minimum.

The Gibb's free energy (ΔG) of the ligand KL and the organotin(IV) carboxylates **1** and **3** were determined using the equation given below:

$$\Delta G = -RT \ln K$$

where “ R ” is the general gas constant ($8.314 \text{ J K}^{-1} \text{ mol}^{-1}$) and T is the temperature (298 K). The Gibb's free energies were found to be -17.15 , -10.27 and $-19.60 \text{ kJ mol}^{-1}$ for KL, **1** and **3**, respectively, indicating the interaction of the complexes with DNA is a spontaneous process.

3.6. Biological activities

3.6.1. Antibacterial activity

In vitro biological screening tests of the synthesized ligand KL and its organotin(IV) complexes were carried out against three gram-positive [*Bacillus subtilis* (ATCC 6633), food poisoning; *Staphylococcus aureus* (ATCC 6538), food poisoning, scaled skin syndrome, endocarditis, *Micrococcus luteus* (ATCC 53598), recurrent bacteremia, septic shock, septic arthritis, endocarditis, meningitis and cavitating pneumonia] and two gram-negative bacteria [*Escherichia coli*, (ATCC 15224), infection of wounds, urinary tract and dysentery; *Bordetella bronchiseptica* (ATCC 4617), atrophic rhinitis] and the results have been summarized in Table 6. The experiment was performed in triplicate by the agar well diffusion method [44]. Cefixime was used as a positive control. The microorganism against which complex 3 presented the highest activity was *B. subtilis*, followed by *B. bronchiseptica* and *S. aureus*. Complex 5 was active against all the tested bacteria except *B. bronchiseptica*, with the best activity of the complex being recorded against *E. coli*, followed by *S. aureus* and *M. luteus*. Complex 1 presented low activity against all bacterial strains. Complexes 2 and 4 were active against Gram-positive bacteria compared with gram-negative bacteria. The results show that the organotin complexes are more potent bactericides than the free ligand. This can be explained in terms of the greater lipid solubility and cellular penetration of the metal complexes [45]. It is observed that the antibacterial activity is enhanced upon coordination of the ligand to the metal, which reduces the polar nature of the tin atom by delocalization of electrons and sharing of charge (positive) with the donor group [46]. Thus, the lipophilic nature of the tin atom increases, which enhances the permeability of the complexes through the plasma membrane.

3.6.2. Antifungal activity

The antifungal activity of the ligand and complexes was recorded against five fungal strains, *Fusarium solani*, *Aspergillus niger*, *Mucor specie*, *Helminthosporium solani* and *Aspergillus flavus* using the agar dilution method [44]. Terbinafine was used as a standard drug in this assay. The results are shown in Table 7. In comparison to the ligand, the complexes were found to be more active toward fungal strains, with a few exceptions, and in some cases their activity is equal to the standard drug which suggests that coordination to metal enhanced the activity as compare to the free ligand. Complexes 4 and 5 show 100% growth inhibition against all fungal strains, whereas complexes 1 and 2 showed $\geq 90\%$ growth inhibition against only one fungal strain (Table 7). Although the exact biochemical mechanism is not completely understood, the mode of action of antimicrobials may involve various targets in the microorganisms. These targets include the following: (1) the higher activity of the metal complexes may be due to the different properties of the metal ions upon chelation. The polarity of the metal ions will be reduced due to the overlapping of ligand orbitals and partial sharing of the positive charge of the metal ion with donor groups. Thus, chelation increases the penetration of the complexes into lipid membranes and the

Table 4
Selected geometric parameters of the optimized structures of complexes **1–5**.

Compd. no.	Bond distance (Å)		Bond angle (°)		Torsion angle (°)	
1	Sn1–C2	2.152	C2–Sn1–C4	109.15	C2–Sn1–C4–S5	101.11
	Sn1–S3	2.619	C4–Sn1–S5	101.89	S3–C4–Sn1–S5	153.87
	Sn1–C4	2.152	S3–Sn1–S5	148.21	S3–Sn1–C2–S9	65.38
	Sn1–S5	2.620	Sn1–S3–C6	88.96	Sn1–S5–C7–O10	178.20
	Sn1–S11	2.846	Sn1–S5–C7	88.95	S3–C6–S9–Sn1	2.05
	S5–C7	1.730	S5–C7–S11	122.21	S3–S9–C6–O8	179.55
2	Sn1–C2	2.173	C2–Sn1–C4	111.55	C2–Sn1–C4–S5	101.20
	Sn1–S3	2.630	C4–Sn1–S5	98.94	S3–C4–Sn1–S5	153.48
	Sn1–C4	2.173	S3–Sn1–S5	148.08	S3–Sn1–C2–S9	64.90
	Sn1–S5	2.632	Sn1–S3–C6	88.78	Sn1–S5–C7–O10	177.80
	Sn1–S11	2.851	Sn1–S5–C7	88.80	S3–C6–S9–Sn1	3.14
	S5–C7	1.730	S5–C7–S11	122.44	S3–S9–C6–O8	179.53
3	Sn1–C2	2.151	C2–Sn1–C4	105.59	C2–Sn1–C4–S5	100.52
	Sn1–S3	2.606	C4–Sn1–S5	101.67	S3–C4–Sn1–S5	155.23
	Sn1–C4	2.151	S3–Sn1–S5	149.08	S3–Sn1–C2–S9	66.30
	Sn1–S5	2.608	Sn1–S3–C6	88.55	Sn1–S5–C7–O10	177.87
	Sn1–S11	2.819	Sn1–S5–C7	88.43	S3–C6–S9–Sn1	2.34
	S5–C7	1.730	S5–C7–S11	122.20	S3–S9–C6–O8	179.63
4	Sn1–C2	2.157	Sn1–S3–C6	102.98	S3–Sn1–C2–C5	127.16
	Sn1–S3	2.501	S3–C6–O7	126.84	C2–Sn1–C4–C5	129.74
	Sn1–C4	2.165	S3–C6–O7	108.29	C2–S3–Sn1–C6	65.16
	Sn1–C5	2.157	C2–Sn1–C5	116.39	S3–C6–S8–O7	179.99
	S3–C6	1.768	S3–Sn1–C5	110.45	S8–O7–C6–C9	0.01
	C6–S8	1.666	S3–Sn1–C4	97.37	C6–O7–C9–C10	179.93
5	Sn1–C2	2.129	Sn1–S3–C6	102.77	S3–Sn1–C2–C5	133.82
	Sn1–S3	2.489	S3–C6–S8	126.56	C2–Sn1–C4–C5	125.24
	Sn1–C4	2.144	S3–C6–O7	108.28	C2–S3–Sn1–C6	63.69
	Sn1–C5	2.136	C2–Sn1–C5	114.67	S3–C6–S8–O7	179.35
	S3–C6	1.769	S3–Sn1–C5	115.36	S8–C6–O7–C9	0.04
	C6–S8	1.662	S3–Sn1–C4	95.95	C6–O7–C9–C10	179.64

blockage of metal binding sites in the enzymes of the microorganisms. (2) Interference with the synthesis of cellular walls, causing damage that can lead to a change in the cell permeability characteristics or disordered lipoprotein arrangements, finally results in cell death [45].

3.6.3. Antileishmanial activity

The ligand KL and its complexes **1–5** were screened against the pathogenic *Leishmania major* using Amphotericin B ($0.048 \mu\text{g mL}^{-1}$) as a standard drug and the data have been summarized in Table 8. All the studied organotin(IV) complexes were more active than the free ligand, confirming the active role of Sn in the antileishmanial activity. The activity reduces in the order: Bu_3SnL (**4**) > Ph_3SnL (**5**) > Ph_2SnL_2 (**3**) > Me_2SnL_2 (**1**) > Bu_2SnL_2 (**2**). According to previous literature [47], the antileishmanial activity is governed by planarity, lipophilicity and low-molecular weight. However, the higher activity of Bu_3SnL (**4**) in the tested series could probably be explained on the basis of the geometry around the tin atom. Four-coordinated Bu_3SnL (**4**) was more active than the five and six-coordinated complexes. The higher activities of complexes **5** and **3** are due to the planar phenyl groups that can penetrate more easily into the lipid bilayer. In some cases, diorganotin complexes were found to be more active, as was observed in the present study in that complex **1** is more active than complex **2** due to the dominating diffusive nature of the small methyl group. Although all the complexes have the potential to be used as drugs, Bu_3SnL (**4**) is a leading candidate in this connection due to its higher activity and minimum cytotoxicity, with an LD_{50} value of $0.001 \mu\text{g mL}^{-1}$. These complexes, especially the last one, may emerge as a novel class of antileishmanial drug, alone or in combination with some other drugs.

3.6.4. Antioxidant activity

The antioxidant abilities of the synthesized ligand and organotin(IV) complexes were determined by their interaction with the free stable radical 1,1-diphenyl-2-picryl-hydrazyl (DPPH) at different concentrations employing a well-known method [48]. Due to its odd electron, DPPH gives a strong absorption band at 517 nm, appearing as a deep violet color [49]. As this electron becomes paired off in the presence of a free radical scavenger, the absorption disappears and the resulting decolorization is stoichiometric with respect to the number of electrons taken up. The change of absorbance produced in this reaction is monitored to calculate the antioxidant potential of the test samples [48]. DPPH is a stable free radical (due to extensive delocalization of the unpaired electron), having λ_{max} at 517 nm. When this radical takes a hydrogen radical from a ligand, the absorption vanishes due to the absence of free electron delocalization [50,51]. By increasing the concentration of the test samples, the absorption intensity of the radical vanishes rapidly at 517 nm. The effect of the ligand and its organotin(IV) complexes have been shown in Table 9 with a comparison to the standard antioxidant ascorbic acid. It was revealed that the tested complexes showed moderate behavior as antioxidants as compared to the standard drug used.

3.6.5. Cytotoxicity

A cytotoxicity assay of the newly synthesized complexes is considered as a useful tool for an initial assessment of their toxicity. Therefore the cytotoxicity of all the synthesized compounds in the present study was checked by a brine-shrimp assay and the results are summarized in Table 10. The cytotoxicity is considered significant if the LD_{50} value is less than 20–30 $\mu\text{g/mL}$ [52,53]. The highest toxicity was observed for complexes **4** and **5**, with LD_{50} values <10 $\mu\text{g/mL}$, while the lowest toxicity was observed for complexes **2** and **3**. The tri-organotin derivatives were found to be

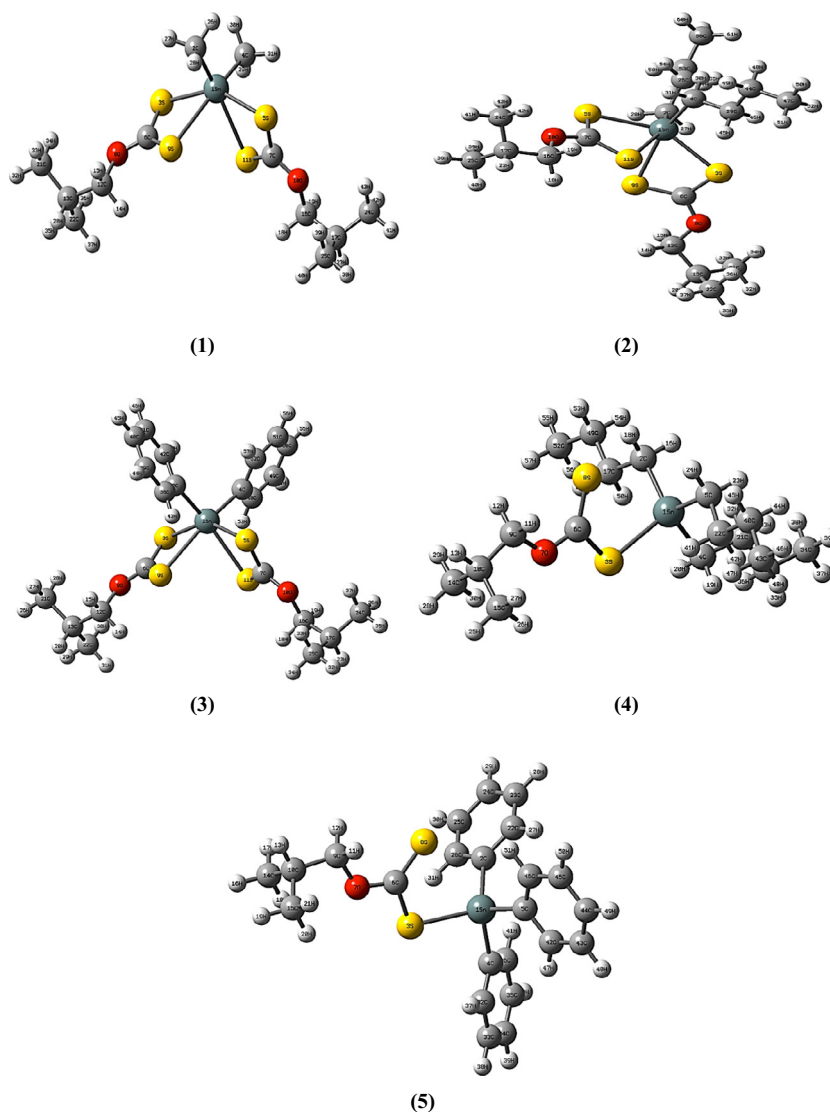


Fig. 4. Optimized molecular structures of complexes 1–5.

more toxic than the di-organotin derivatives and the ligand, which is in accordance with our earlier study [58].

3.6.6. Protein kinase inhibition activity

The data in Table 11 shows that complexes 1–5 have varying degrees of inhibition, producing zones of inhibition ranging from 6.0 to 12.0 mm as compared to the standard's value of 18 mm. The exact mechanism is still not known, but it is proposed that the aerial hyphae formation of *Streptomyces species* is blocked, thus it may be hypothesized that it inhibits cancer cell proliferation [54]. Complex 4 was found to be the most effective as it produced the maximum zone of inhibition on the culture plates and it may be considered as a potential candidate to inhibit tumor initiation.

3.7. Structure activity relationship

The structure–activity relationship is required to understand the relationship between the structure and biological activity of complexes. Organotin(IV) complexes display a broad spectrum of biological effects and have been extensively studied as bactericides, fungicides, wood preservatives, antitumor and anticancer agents [55–57]. The biological activities may depend on

substitution on the ligand and organic groups attached to tin [58]. To correlate the structures and activities of the synthesized complexes 1–5, it is observed that variation in the toxicity of different antibacterial agents against different organisms depends either on the impermeability of the cell or differences in the ribosomes to the antimicrobial agent. Though the present results suggest that the synthesized organotin(IV) complexes inhibit the growth of organisms to a greater extent, which is in accordance with earlier reports [59], among the synthesized organotin complexes, tri-organotin(IV) complexes, i.e. 4 and 5, showed higher activity as compared to the diorganotin(IV) complexes 1–3. The greater activity may be attributed to the higher solubility of the complexes. Also theoretical calculations have been used to study the structure–activity relationship (SAR); we have calculated the energies of the HOMO and LUMO orbitals. The difference between the energies of the HOMO and LUMO (the HOMO–LUMO gap) shows the stability or reactivity of the molecules, pointing out the possible biological receptors in the complexes, such as electron rich or electron deficient regions. The lipophilic nature of the complexes can be evaluated by the logarithm of the partition coefficient (LogP), which indicates the ability of the molecule to overcome biological barriers and move into different biophases.

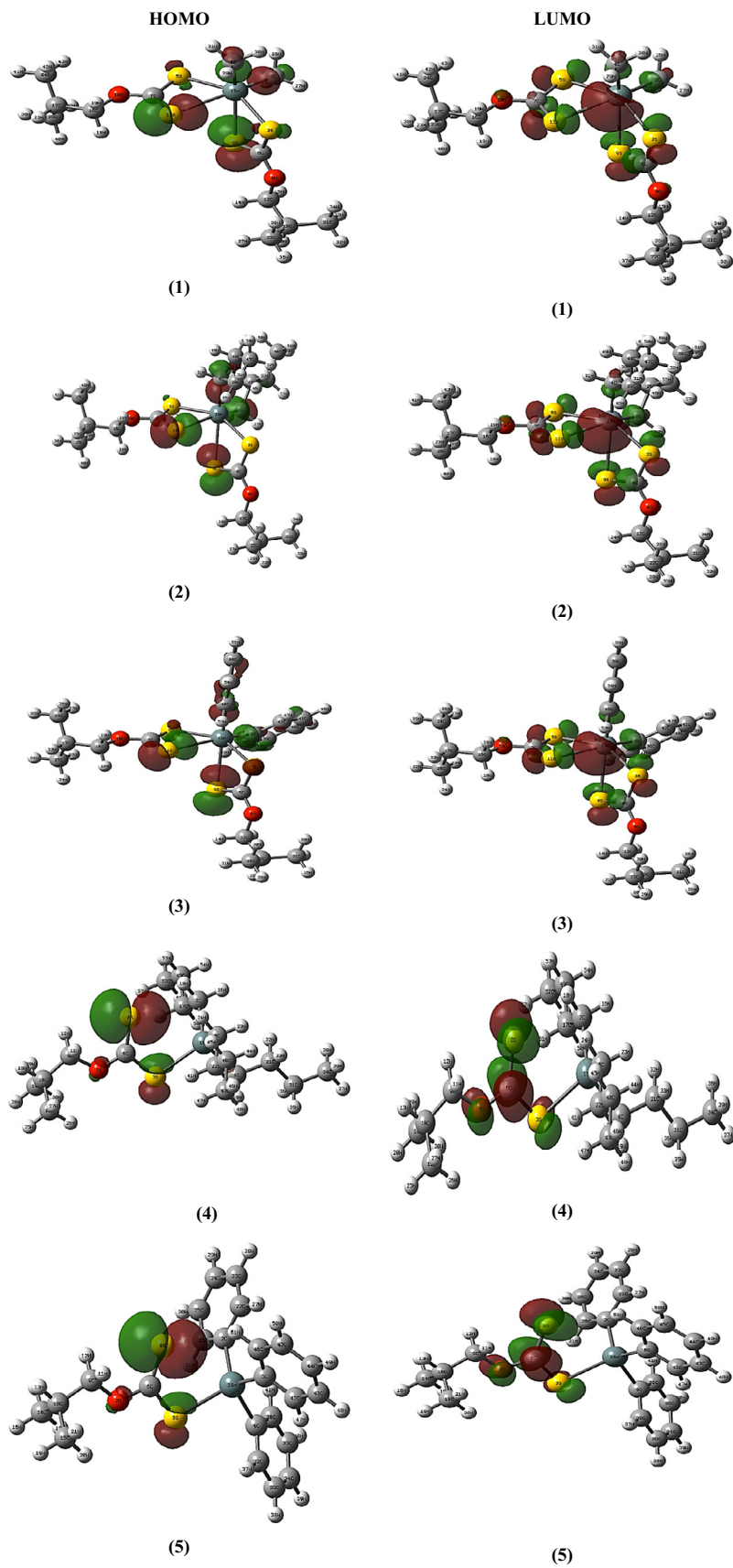


Fig. 5. Optimized HOMO and LUMO orbitals of complexes 1–5.

Table 5
Energies of the HOMO and LUMO of complexes 1–5 calculated with DFT/B3LYP.

Compd. no.	HOMO (eV)	LUMO (eV)	HOMO–LUMO gap (eV)
1	–6.33426	–1.73445	4.59981
2	–6.12120	–1.63758	4.48362
3	–6.38569	–1.74234	4.64335
4	–5.97235	–1.08410	4.88825
5	–6.03603	–1.14940	4.88663

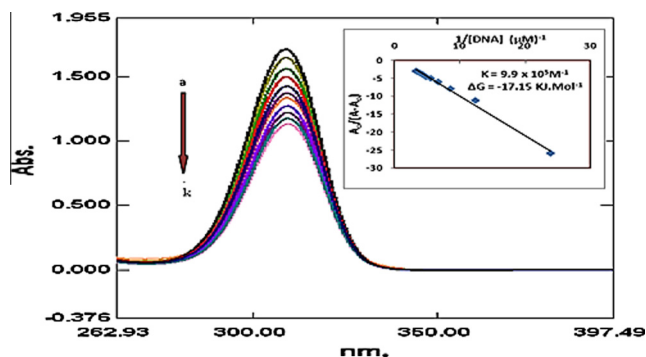


Fig. 6. UV–Vis spectra of 0.8 mmol L^{-1} complex KL in the absence and presence of (a) 20 (b) 40 (c) 62 (d) 83 (e) 104 (f) 125 (g) 150 (h) 170 (i) 192 (j) and 222 (k) μM DNA.

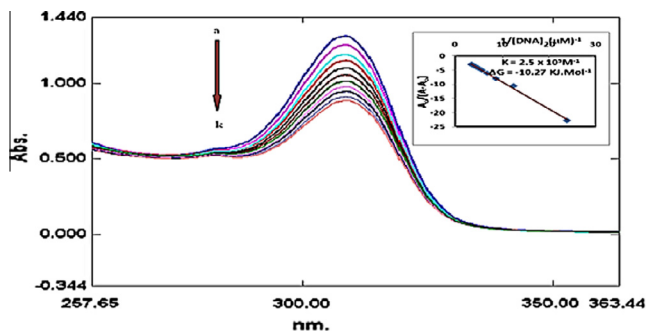


Fig. 7. UV–Vis spectra of 0.8 mmol L^{-1} Me_2SnL_2 (1) in the absence and presence of (a) 20 (b) 40 (c) 62 (d) 83 (e) 104 (f) 125 (g) 150 (h) 170 (i) 192 (j) and 222 (k) μM DNA.

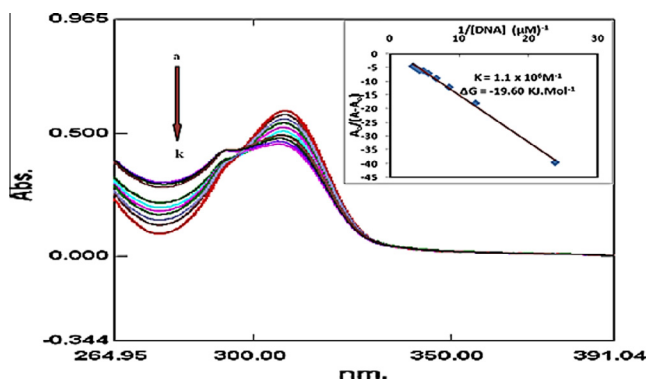


Fig. 8. UV–Vis spectra of 0.8 mmol L^{-1} Ph_2SnL_2 (3) in the absence and presence of (a) 20 (b) 40 (c) 62 (d) 83 (e) 104 (f) 125 (g) 150 (h) 170 (i) 192 (j) and 222 (k) μM DNA.

Table 6
Antibacterial data of KL and the organotin(IV) complexes 1–5.

Compd. no.	Zone of inhibition (mm)				
	<i>B. subtilis</i>	<i>M. luteus</i>	<i>S. aureus</i>	<i>E. coli</i>	<i>B. bronchiseptica</i>
KL	11	12	–	–	10
1	15	10	11	9	15
2	19	14	–	9	–
3	26	15	19	11	24
4	17	14	10	9	–
5	18	29	28	22	10
Cefixime	29	32	35	37	30

Table 7
Antifungal data of KL and the organotin(IV) complexes 1–5.

Compd. no.	% growth inhibition				
	<i>F. solani</i>	<i>A. niger</i>	<i>M. specie</i>	<i>H. solani</i>	<i>A. flavus</i>
KL	0	0	0	0	40
1	0	0	70	75	90
2	0	25	30	25	100
3	0	30	75	20	30
4	100	100	100	100	100
5	100	100	100	100	100
Turbinafine	100	100	100	100	100
DMSO	0	0	0	0	0

Table 8
Antileishmanial data of KL and the organotin(IV) complexes 1–5.

Compd. no.	LC_{50} ($\mu\text{g/mL}$)
KL	3.89
1	0.031
2	0.666
3	0.031
4	0.001
5	0.002
Amphotericin B	0.048

Table 9
Antioxidant data of KL and the organotin(IV) complexes 1–5.

Compd. No.	IC_{50} ($\mu\text{g/mL}$)
KL	0.67
1	0.95
2	2.52
3	0.56
4	1.70
5	1.95
Ascorbic acid	0.49

Table 10
Cytotoxicity data of KL and the organotin(IV) complexes 1–5.

Compd. no.	No of shrimps killed out of 20 per dilution			
	100 $\mu\text{g/mL}$	50 $\mu\text{g/mL}$	10 $\mu\text{g/mL}$	LD_{50}
KL	18	11	9	16.43
1	19	16	11	8.254
2	11	10	6	58.2
3	17	10	5	34.6
4	20	20	20	<10
5	20	20	20	<10

Table 11
Protein kinase inhibition data of organotin(IV) complexes 1–5.

Compd. no.	Zone of inhibition (mm) \pm SD
1	11 \pm 0.5
2	6 \pm 0.5
3	11 \pm 0.6
4	12 \pm 1.1
5	8 \pm 0.5
Tyrab	18

4. Conclusions

Potassium *o*-isobutyl carbonodithioate and its organotin(IV) complexes were successfully synthesized and characterized. The potassium salt was treated with different di- and triorganotin(IV) chlorides to form the corresponding organotin(IV) complexes. The UV–Vis spectroscopic results show that the synthesized complexes bind to DNA *via* the intercalative mode of interaction, resulting in hypochromism with a minor red shift. The negative values of the Gibbs's free energy change show the spontaneity of these interactions. HOMO–LUMO calculations show that all the complexes are thermodynamically stable. Biological activity data revealed that the complexes were more active than the free ligand, with a few exceptions, and were found to be active in their biological action.

Acknowledgments

The authors are thankful to the Higher Education Commission Pakistan for financial support.

A. Supplementary data

CCDC 1062080 contains the supplementary crystallographic data for complex 1. These data can be obtained free of charge via <http://www.ccdc.cam.ac.uk/conts/retrieving.html>, or from the Cambridge Crystallographic Data Centre, 12 Union Road, Cambridge CB2 1EZ, UK; fax: (+44) 1223-336-033; or e-mail: deposit@ccdc.cam.ac.uk. Supplementary data associated with this article can be found, in the online version, at <http://dx.doi.org/10.1016/j.poly.2015.11.041>.

References

- [1] J.D. Wilton-Ely, D. Solanki, E.R. Knight, K.B. Holt, A.L. Thompson, G. Hogarth, *Inorg. Chem.* 47 (20) (2008) 9642.
- [2] N. Srinivasan, S. Thirumaran, S. Ciattini, *J. Mol. Struct.* 921 (1) (2009) 63.
- [3] S. Shahzadi, S. Ali, *J. Iranian Chem. Soc.* 5 (1) (2008) 16.
- [4] A.T. Kana, T.G. Hibbert, M.F. Mahon, K.C. Molloy, I.P. Parkin, L.S. Price, *Polyhedron* 20 (24) (2001) 2989.
- [5] G. Hogarth, *Mini-Rev. Med. Chem.* 12 (12) (2012) 1202.
- [6] Z.U. Rehman, S. Shahzadi, S. Ali, G.X. Jin, *Turk. J. Chem.* 31 (4) (2007) 435.
- [7] Z.U. Rehman, M.M. Barsan, I. Wharf, N. Muhammad, S. Ali, A. Meetsma, I.S. Butler, *Inorg. Chim. Acta* 361 (11) (2008) 3322.
- [8] E.R. Tiekink, I. Haiduc, *Prog. Inorg. Chem.* 54 (2005) 127.
- [9] K. Xu, W. Ding, *Mater. Lett.* 62 (29) (2008) 4437.
- [10] Q. Han, J. Chen, X. Yang, L. Lu, X. Wang, *J. Phys. Chem. C* 111 (38) (2007) 14072.
- [11] D.E. Zelmon, Z. Gebeyehu, D. Tomlin, T.M. Cooper, T. M. in: *MRS Proceedings* (1998) Vol. 519, p. 395. Cambridge University Press.
- [12] N. Kalgotra, B. Gupta, K. Kumar, S.K. Pandey, *Phosphorus, Sulfur Silicon Relat. Elem.* 187 (3) (2012) 364.
- [13] E.I. Stout, B.S. Shasha, W.M. Doane, *J. Appl. Polym. Sci.* 24 (1) (1979) 153.
- [14] M. Scendo, *Corros. Sci.* 47 (7) (2005) 1738.
- [15] W.J. Orts, R.E. Sojka, G.M. Glenn, *Agro Food Industry Hi-Tech* 13 (4) (2002) 37.
- [16] O.A. Görgülü, M. Arslan, E. Çil, *J. Coord. Chem.* 59 (6) (2006) 637.
- [17] A.C. Larsson, S. Öberg, *J. Phys. Chem. A* 115 (8) (2011) 1396.
- [18] E. Amtmann, *Drugs Exp. Clin. Res.* 22 (6) (1995) 287.
- [19] M. Perluigi, G. Joshi, R. Sultana, V. Calabrese, C. De Marco, R. Coccia, D.A. Butterfield, *Neuroscience* 138 (4) (2006) 1161.
- [20] M. Sirajuddin, S. Ali, V. McKee, M. Sohail, H. Pasha, *Eur. J. Med. Chem.* 84 (2014) 343.
- [21] M. Sirajuddin, S. Ali, V. McKee, S. Zaib, J. Iqbal, *RSC Adv.* 4 (2014) 57505.
- [22] W.L. Armarego, C. Chai, *Purification of Laboratory Chemicals*, Butterworth-Heinemann, 2012.
- [23] M.J. Frisch, G.W. Trucks, H.B. Schlegel, G.E. Scuseria, M.A. Robb, J.R. Cheeseman, V.G. Zakrzewski, Gaussian suite Gaussian 03, Revision C. 01, Gaussian Inc., Wallingford CT, 2004.
- [24] G. Schaftenaar, J.H. Noordik, *J. Comput. Aided Mol. Des.* 14 (2) (2000) 123.
- [25] J. Thomas, P. Sherwood, CCP1–GUI, a general-purpose visualization code for electronic structure codes. Version 0.8 (2010).
- [26] M. Sirajuddin, S. Ali, N.A. Shah, M.R. Khan, M.N. Tahir, *Spectrochim. Acta Part A Mol. Biomol. Spectrosc.* 94 (2012) 134.
- [27] F. Javed, S. Ali, M.W. Shah, K.S. Munawar, S. Shahzadi, Hameedullah, H. Fatima, M. Ahmed, K. Saroj, S.K. Sharma, K. Qanungo, *J. Coord. Chem.* 67 (16) (2014) 2795.
- [28] F. Shaheen, S. Ali, A. Meetsma, *Polyhedron* 31 (1) (2012) 697.
- [29] O.S. Jung, Y.S. Sohn, J.A. Ibers, *Inorg. Chem.* 25 (13) (1986) 2273.
- [30] G. Domazetis, R.J. Magee, B.D. James, *J. Organomet. Chem.* 141 (1) (1977) 57.
- [31] S. Shahzadi, S. Ali, K. Wurst, M. Najam-ul-Haq, *Heteroat. Chem.* 18 (6) (2007) 664.
- [32] T.P. Lockhart, W.F. Manders, E.M. Holt, *J. Am. Chem. Soc.* 108 (21) (1986) 6611.
- [33] R. Willem, I. Verbruggen, M. Gielen, M. Biesemans, B. Mahieu, T.S. Basu Baul, E. R. Tiekink, *Organometallics* 17 (26) (1998) 5758.
- [34] M.I. Mohamed-Ibrahim, S.S. Chee, M.A. Buntine, M.J. Cox, E.R. Tiekink, *Organometallics* 19 (25) (2000) 5410.
- [35] S. Ali, N. Muhammed, A. Meetsma, *Acta Crystallogr., Sect. E: Struct. Rep. Online* 63 (2) (2007) m431.
- [36] T. Zöllner, L. Iovkova-Berends, T. Berends, C. Dietz, G. Bradtmöller, K. Jurkschat, *Inorg. Chem.* 50 (17) (2011) 8645.
- [37] I. Pal, F. Basuli, S. Bhattacharya, *J. Chem. Sci.* 114 (4) (2002) 255.
- [38] A.K. Mishra, N. Manav, N.K. Kaushik, *Spectrochim. Acta Part A Mol. Biomol. Spectrosc.* 61 (13) (2005) 3097.
- [39] X. Yang, G.L. Shen, R.Q. Yu, *Microchem. J.* 62 (3) (1999) 394.
- [40] N. Shahabadi, S. Mohammadi, R. Alizadeh, *Bioinorg. Chem. Appl.* (2011).
- [41] K. Ghosh, P. Kumar, N. Tyagi, U.P. Singh, V. Aggarwal, M.C. Baratto, *Eur. J. Med. Chem.* 45 (9) (2010) 3770.
- [42] K. Ghosh, P. Kumar, N. Tyagi, *Inorg. Chim. Acta* 375 (1) (2011) 77.
- [43] H.A. Benesi, J.H. Hildebrand, *J. Am. Chem. Soc.* 71 (8) (1949) 2703.
- [44] T.R. Fritsche, P.F. McDermott, T.R. Shryock, R.D. Walker, *J. Clin. Microbiol.* 45 (8) (2007) 2758.
- [45] Y. Anjaneyulu, R.P. Rao, *Synth. React. Inorg. Met.-Org. Chem.* 16 (2) (1986) 257.
- [46] Z.U. Rehman, N. Muhammad, A. Shah, S. Ali, E. Khan, *Heteroat. Chem.* 23 (6) (2012) 560.
- [47] B. Raychaudhury, S. Banerjee, S. Gupta, R.V. Singh, S.C. Datta, *Acta Trop.* 95 (1) (2005) 1.
- [48] D.N. Nicolaides, D.R. Gautam, K.E. Litinas, D.J. Hadjipavlou-Litina, K.C. Fylaktakidou, *Eur. J. Med. Chem.* 39 (4) (2004) 323.
- [49] T. Kulisic, A. Radonic, V. Katalinic, M. Milos, *Food Chem.* 85 (4) (2004) 633.
- [50] C. Kontogiorgis, D. Hadjipavlou-Litina, *J. Enzym. Inhib. Med. Chem.* 18 (1) (2005) 63.
- [51] M.C. Foti, C. Daquino, C. Geraci, *J. Org. Chem.* 69 (7) (2004) 2309.
- [52] A.J. Crowe, P.J. Smith, G. Atassi, *Inorg. Chim. Acta* 93 (4) (1984) 179.
- [53] S.U. Rehman, S. Ali, A. Badshah, A. Malik, E. Ahmed, G.X. Jin, E.R. Tiekink, *Appl. Organomet. Chem.* 18 (8) (2004) 401.
- [54] J. Zhang, P.L. Yang, N.S. Gray, *Nat. Rev. Cancer* 9 (1) (2009) 28.
- [55] G. Eng, D. Whalen, P. Musingarimi, J. Tierney, M. DeRosa, *Appl. Organomet. Chem.* 12 (1) (1998) 25.
- [56] C. Zhu, L. Yang, D. Li, Q. Zhang, J. Dou, D. Wang, *Inorg. Chim. Acta* 375 (1) (2011) 150.
- [57] M. Gielen, M. Biesemans, D. de Vos, R. Willem, *J. Inorg. Biochem.* 79 (1) (2000) 139.
- [58] M. Tariq, S. Ali, N. Muhammad, N.A. Shah, M. Sirajuddin, M.N. Tahir, N. Khalid, M.R. Khan, *J. Coord. Chem.* 67 (2) (2014) 323.
- [59] Z. Rehman, N. Muhammad, S. Ali, I.S. Butler, A. Meetsma, *Inorg. Chim. Acta* 373 (1) (2011) 187.
- [60] H.L. Singh, J.B. Singh, S. Bhanuka, *Res. Chem. Intermed.* (2015) 1.